

# Liquid Crystal Elastomers with Magnetic Actuation

Moritz Winkler,<sup>1</sup> Andreas Kaiser,<sup>1</sup> Simon Krause,<sup>2</sup> Heino Finkelmann,<sup>2</sup>  
Annette M. Schmidt<sup>\*1</sup>

**Summary:** Magneto-active liquid crystal elastomers (LCEs) are accessible by the incorporation of superparamagnetic  $\text{Fe}_3\text{O}_4$  nanoparticles into oriented nematic side-chain LCEs and offer a contactless activation pathway to the nematic-to-isotrope transition by local magnetic heating in external fields. In magneto-mechanical measurements, a sample contraction of up to 30% is observed under field influence, with full reversibility when the field is switched off. The load evolved reaches 60 kPa and more. The ability of the materials to respond to a contactless electromagnetic stimulus with a well-defined contraction can be of use for various actuator applications.

**Keywords:** actuators; liquid crystalline polymers (LCP); magnetic polymers; nanocomposites; stimuli-sensitive polymers

## Introduction

Liquid crystal elastomers (LCEs) offer an interesting spectrum of properties, including temperature-induced, fully-reversible shape changes connected with considerable development of pulling force, and synthetic diversity. The covalent linking of mesogenic units to a crosslinked three-dimensional structure results in a coupling of the macroscopic properties, such as shape and strain, to the microscopic structure dominated by the order and degree of orientation of the mesogens. As a consequence, anisotropic (monodomain) LCEs exhibit a dramatic shape change at the nematic-isotropic phase transition of the liquid crystalline phase, as was predicted by De Gennes<sup>[1]</sup> and experimentally confirmed in 1991.<sup>[2]</sup> As this is a thermodynamic equilibrium phenomenon, the process is fully reversible.

However, to turn the unusual properties of LCEs in a viable device, it is desirable to trigger such shape changes with other stimuli rather than temperature changes. Next to practical implications of temperature changes, e.g. in biological systems, the need for a fast response time limits the applicability of LCEs operated by temperature, with response times that are generally ruled by heat conductivity and sample size.

In order to take advantage of LCEs for an extended number of viable devices, it is desirable to trigger such shape changes with electromagnetic fields rather than external temperature changes.<sup>[4–9]</sup> Some of the limitations can be readily faced by the use of magnetic nanoparticles (MNP) as antennas for electromagnetic energy dissipation.

MNPs are known to transfer energy from electro-magnetic irradiation into heat due to relaxation processes.<sup>[10,11]</sup> This behavior offers the possibility to induce phase changes locally in the environment of the particles by using AC fields in the kHz range,<sup>[12–15]</sup> a frequency range where many other materials are transparent. Recently, the applicability of magnetic heating by iron oxide nanoparticles has been demonstrated for shape memory thermosets.<sup>[16]</sup>

<sup>1</sup> Institut für Organische Chemie und Makromolekulare Chemie, Heinrich-Heine-Universität Düsseldorf, Universitätsstr. 1, D-40225 Düsseldorf, Germany  
Fax: (+49) 211 8115840;

E-mail: Schmidt.annette@uni-duesseldorf.de

<sup>2</sup> Institut für Makromolekulare Chemie, Albert-Ludwigs-Universität Freiburg, Stefan-Meier-Str. 31, D-79104 Freiburg, Germany

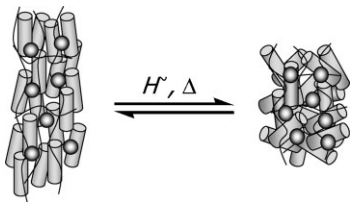
**Scheme 1.**

Illustration showing the magnetically-induced length contraction in magneto-active LCEs. Scales do not apply.

Magneto-active LCEs are accessible by the incorporation of superparamagnetic  $\text{Fe}_3\text{O}_4$  nanoparticles into oriented nematic side-chain LCEs and offer a contactless activation pathway to the nematic-to-isotrope transition by local magnetic heating.

## Experimental Part

Transmission electron microscopy (TEM) images were recorded with a LEO 912 Omega TEM. Sample preparation was carried out with a Leica Ultracut UCT equipped with a cryo chamber Leica EM FCS at  $-120^\circ\text{C}$ .

X-Ray diffraction measurements were performed using monochromatic  $\text{CuK}\alpha$  irradiation ( $\lambda = 1.54 \text{ \AA}$ ) and a two-dimensional image plate detector system.

VSM was recorded on a magnetometer EV7 (ADE magnetics) with a field maximum of  $1.3 \times 10^6 \text{ A m}^{-1}$ .

Thermal properties of the LCEs were analysed by DSC. The system used was a Mettler Toledo DSC 822<sup>e</sup> equipped with a sample robot TSO801RO. Samples were measured between  $-50^\circ\text{C}$  and  $150^\circ\text{C}$  with a heating rate of  $10 \text{ K min}^{-1}$ .

Magnetic heating experiments were performed on a Huettinger High Frequency (HF) Generator TIG 5.0/300 with a copper inductor ( $l = 50 \text{ mm}$ ,  $d_l = 35 \text{ mm}$ ,  $n = 5$ ). The apparatus was operated at  $300 \text{ kHz}$  at a maximum induction power of  $5.0 \text{ kW}$  and a maximum amplitude field strength  $H \sim$  of  $42.6 \text{ kA m}^{-1}$ . The tempera-

ture was recorded with an Opsens OTG-A fibre optic system.

Mechanical characteristics of the LCEs were investigated with a Zwick-Roell tensile-strength tester TC-FR2.5 equipped with a thermobox W91300. For magneto-mechanical experiments, the tensile-strength tester was combined with the HF generator. The tested LCE is placed in the middle of the copper inductor with non-metal clamps, in order to avoid clamp heating under the field influence. Relative sample length was recorded while the sample stress  $\sigma$  was kept constant at a value of  $\sigma = 0 \text{ kPa}$ .

## Synthesis of the Toluene-Based Magnetic Fluid (MF)

The synthesis of the magnetic fluid is realized by the precipitation of magnetite ( $\text{Fe}_3\text{O}_4$ ) nanoparticles by alkaline hydrolysis of ferrous and ferric chloride (molar ratio 1:2)<sup>[17]</sup> and followed by stabilization of the particles in toluene with *N*-oleoylsarcosine by a recently published method.<sup>[18]</sup> The  $\text{Fe}_3\text{O}_4$  content of the dispersions is determined by vibrating sample magnetometry (VSM) to  $0.5 \text{ vol\%}$ . The resulting stable particle dispersion (magnetic fluid, MF) is used as the medium in the synthesis of liquid crystal elastomers in order to incorporate  $\text{Fe}_3\text{O}_4$  particles to the polymer network.

## Synthesis of Magnetoactive Liquid Crystal Elastomer Nanocomposites

The synthesis of magneto-active LCE networks is carried out in analogy to the two-step crosslinking procedure published earlier for oriented LCEs.<sup>[2,18]</sup> Poly[hydrogen methyl siloxane] as polymer backbone, 4-(3-butenoxy)benzoic acid 4-methoxyphenyl ester as the mesogen and 1,4-bis(undecyl-10-enyloxy)benzene as the crosslinking agent are dissolved in the magnetic fluid containing a predetermined volume fraction of MNP. 1,5-Cyclooctadienyl platinum(II) dichloride as catalyst is added and the dispersion is filled into a mould ( $81 \times 20 \times 2 \text{ mm}^3$ ), which is placed in a drying cabinet for  $80 \text{ min}$  at  $70^\circ\text{C}$ . Afterwards, the mould

is cooled down and then removed. In order to synthesize mono-domain samples, LCE strips are loaded with 3.5 kPa during the final crosslinking process. By variation of the  $\text{Fe}_3\text{O}_4$  concentration in the MF, LCEs with particle content up to 1.8 vol% are obtained.

## Results and Discussion

The incorporation of magnetic nanoparticles into monodomain nematic side-chain LCEs is achieved by the addition of a stable, toluene-based particle dispersion to the crosslinking prepolymer mixture and crosslinking in situ, performed in a two-step crosslinking process in analogy to the procedure published previously for particle-free LCEs.<sup>[2,18]</sup>

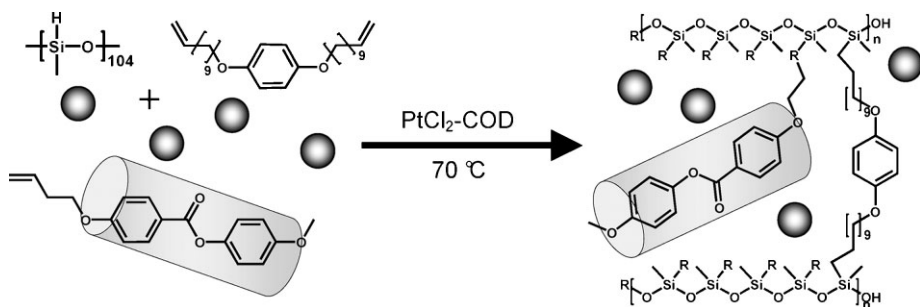
The elastomers consist of a polysiloxane backbone and 4-(3-butenoxy)-benzoic acid 4-methoxy-phenyl ester type LC-side groups. Mesogen, siloxane and the crosslinking agent are added to the MF, and LCEs are prepared by heating the mixture in an appropriate mould to 70 °C. In order to obtain monodomain samples, the slightly crosslinked gels are removed from the mould and loaded with 3.5 kPa during the final crosslinking process at 70 °C. Electron microscopic investigations (TEM) reveal a successful and homogenous incorporation of the magnetic nanoparticles in the LCE samples (Figure 1a).

In order to characterize the stock MF as well as the resulting LCE samples, VSM

measurements are performed (Figure 2a). Assuming a spontaneous magnetization value of  $4.5 \times 10^5 \text{ A m}^{-1}$  for  $\text{Fe}_3\text{O}_4$ , a particle content of  $v_{\text{Fe}_3\text{O}_4} = 0.48 \text{ vol.-%}$  for the stock MF, and a  $\text{Fe}_3\text{O}_4$  content up to 1.64 vol% for magnetic LCE samples are obtained. From initial susceptibility  $\chi_{\text{ini}}$ , an average hydrodynamic core diameter of 11.8 nm can be calculated in agreement with results from TEM. As shown in Figure 1b, typical X-ray diffractograms indicate a mono-domain structure with an order parameter of  $S = 0.63$  that was determined by the method of Mitchell et al.<sup>[19,20]</sup>

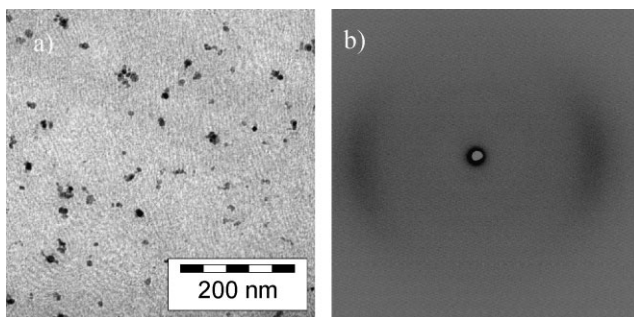
To ensure that the heat development by the incorporated  $\text{Fe}_3\text{O}_4$  particles is sufficient to reach  $T_{\text{NI}}$ , magnetic heating experiments are performed by placing the sample in the center of an induction coil that is fed with a LC circuit, and the sample temperature is recorded versus irradiation time with a fiber optic temperature probe system.

It is observed that the temperature of MNP-containing samples increases with time, and that this increase depends on the  $\text{Fe}_3\text{O}_4$  concentration. The initial heating rate  $(dT/dt)_{\text{ini}}$  increases linearly with the MNP concentration from  $0.44 \text{ K s}^{-1}$  to  $1.81 \text{ K s}^{-1}$ , resulting in a sample temperature up to 95 °C for the highest magnetic material load after 2.5 min under the experimental conditions (Figure 2b). The slope of the linear plot of  $(dT/dt)_{\text{ini}}$  against the MNP concentration delivers the concentration independent specific heating



**Scheme 2.**

Synthesis of magneto-active LCEs by incorporation of magnetic nanoparticles in situ during crosslinking by hydrosilylation.

**Figure 1.**

(a) TEM image and (b) x-ray diffraction pattern of magnetoactive LCEs. (a) polydomain, (b) oriented.

power of the particles immobilized in the LCE matrix,  $P_M = 56.8 \text{ W g}^{-1}$ .

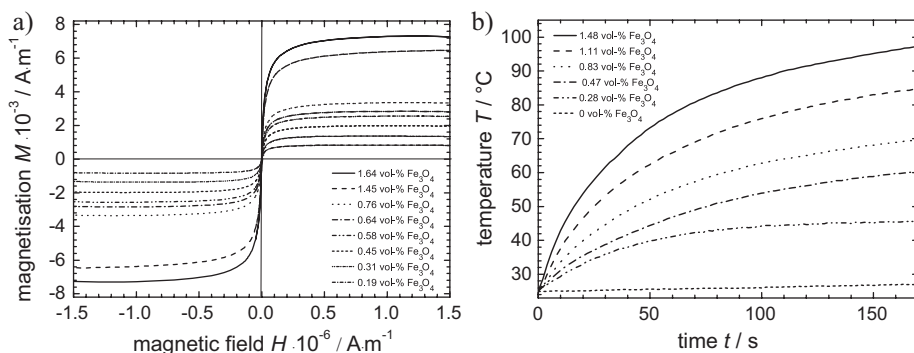
The phase transition temperature  $T_{NI}$  of around  $70^\circ\text{C}$  that does not show influence of the particle concentration is reached for samples with at least 1.4 vol%  $\text{Fe}_3\text{O}_4$  content in this setup. The experiments show that MNP loaded LCEs can be heated sufficiently in order to induce the phase transition in a HF magnetic field.

A detailed theoretical study on the temperature profile development with time has been conducted recently for MNP-filled elastomers under magnetic heating, and the results showed good quantitative agreement with the experimental results presented here.<sup>[21]</sup> The results indicate that a fast regional equilibration can be expected over the sample already at low thermal conductivities of the matrix. In addition, the important impact of the heat transfer to the

sample environment, and thus the sample size on the saturation temperature after reaching the steady state is pointed out.

In order to investigate the mechanical properties of LCEs, a tensile-strength tester is used. The setup can be equipped either with a thermo-chamber, or an induction coil coupled to a HF generator, in order to investigate either the temperature influence in thermo-mechanical experiments, or the impact of the AC field in the magneto-mechanical setup. Cyclic experiments are conducted under constant stress ( $\sigma = 0$ ). By recording temperature and sample length versus time, we obtain information on the fully reversible contraction / expansion of the sample material. Results of the mechanical properties are presented in Table 1.

MNP-loaded LCE samples with particle contents between 0 and 1.64 vol% are analyzed. Sample contractions up to a

**Figure 2.**

(a) Quasi-static magnetization curves and (b) magnetic heating profiles of magneto-active LCEs in AC magnetic fields.

**Table 1.**

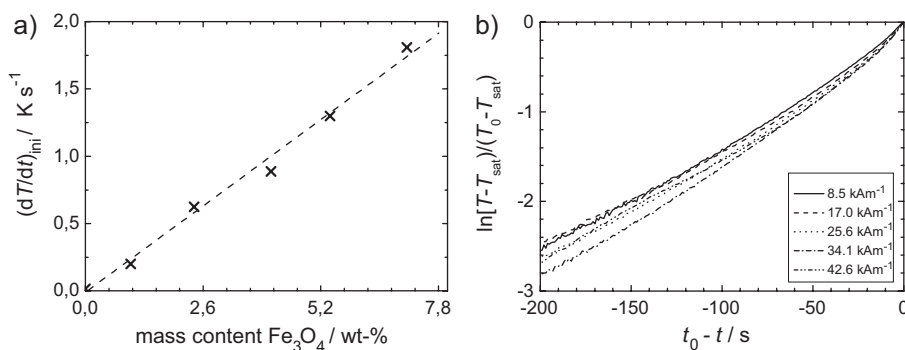
Thermo-mechanical and magneto-mechanical properties of MNP-loaded LCE samples.

Sample <sup>a</sup>	$v_{\text{Fe}_3\text{O}_4}$ <sup>b</sup> [vol%] [b]	$\lambda_T$ <sup>c</sup> [%] [c]	$\lambda_M$ <sup>d</sup> [%] [d]	$(1-\lambda_M)/(1-\lambda_T)$ <sup>e</sup> [%]
Mo@BMP SO	0	76.2	99.7	1.3
Mo2@BMP SO	0.19	79.5	98.1	9.3
Mo3@BMP SO	0.31	68.8	96.0	12.8
Mo6@BMP SO	0.58	79.3	94.7	25.6
Mo8@BMP SO	0.76	74.0	93.7	24.2
M15@BMP SO	1.45	80.6	85.2	76.3
M16@BMP SO	1.64	73.0	74.0	96.3

<sup>a</sup>sample denotations: M( $v_{\text{Fe}_3\text{O}_4} \times 10$ )@LCE. <sup>b</sup> $\text{Fe}_3\text{O}_4$  volume content (VSM). <sup>c</sup>relative sample length  $\lambda_T = L_{80}/L_{25}$ , from sample length at 25 °C ( $L_{25}$ ) and at 80 °C ( $L_{80}$ ). <sup>d</sup>relative sample length  $\lambda_M = L_{\text{on}}/L_{\text{off}}$  from sample length in the absence ( $L_{\text{off}}$ ) and presence ( $L_{\text{on}}$ ) of the HF field (300 kHz, 42.6 kA m<sup>-1</sup>). <sup>e</sup>relative contraction ratio of thermal and magnetical activation.

relative length  $\lambda_T$  of 74% are reached by heating the sample in a thermo-chamber between 25 °C and 80 °C. The achieved contraction is not affected by the particle load, but rather by the mechanical pre-treatment, and full reversibility is observed over at least five heating/cooling cycles. For detailed investigations on the magneto-mechanical behaviour of  $\text{Fe}_3\text{O}_4$  loaded LCE samples, the tensile strength tester is combined with the inductor coil, and the elastomer strips are fixed in the clamps of the instrument, located in the centre of the induction coil. In order to gain information on the reversibility and the velocity of the field-induced shape change, on/off-cycles of various electromagnetic field amplitudes and on samples containing different amounts of MNPs are performed, and the resulting sample length is recorded.

Figure 4a shows the results for magneto-mechanical measurements of LCEs with different MNP amounts at a constant field amplitude  $H$  in dependence of time. After the field is switched on, an immediate contraction of the sample is observed, and the specimen reaches a saturation length in the field after a couple of minutes. The resulting relative sample length  $\lambda_M$  in the presence of the field depends on the particle volume fraction. Values between 99.7% for the LCE sample without any particles, and 74% for the sample with the highest investigated particle load are found. The values can be correlated to the respective contraction behavior by thermal activation by forming the contraction ratio of  $(1-\lambda_M)/(1-\lambda_T)$ . We find that a full contraction comparable to the thermal activation can be found for a material containing

**Figure 3.**

(a) Linear relationship between initial heating rate  $(dT/dt)_{\text{ini}}$  and magnetite content; (b) indication of logarithmic relationship between  $T$  and  $t$ .

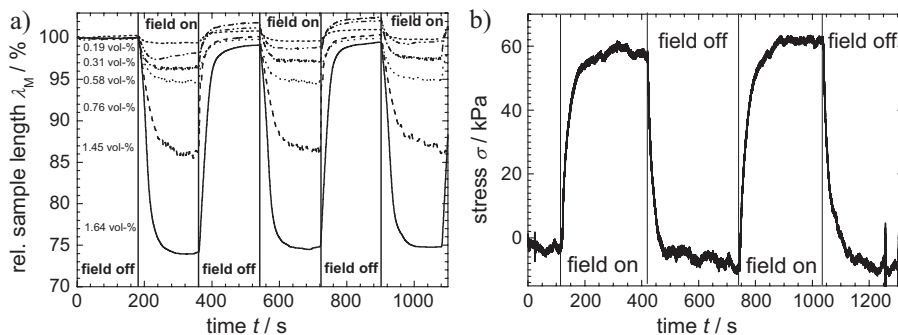


**Figure 4.**

Magnetomechanical behavior of LCEs containing various MNP contents in AC field at 300 kHz,  $43 \text{ kA m}^{-1}$ ; (a) under constant load of  $\sigma = 0$ ; (b) under constant strain ( $v_{Fe_3O_4} = 1.64 \text{ vol}\%$ ).

1.64 vol% of MNP. The cycles show that the observed contraction is reversible, and that  $\lambda_M$  decreases with the applied amount of particles, since the rate of heat development and the maximum sample temperature in the elastomeric sample depends on the particle concentration. In cycles recorded under constant strain, the force developed from the sample is determined to reach 60 kPa and more (Figure 4b).

For the temperature development with time, it is reasonable to expect the following: Due to magnetic heating of the nanoparticles under the field influence, a constant heat flux  $Q_M = P_M \cdot v_{Fe_3O_4}$  is generated within the sample when the field is switched on. An ideally-isolated sample would show a constant heating rate  $dT/dt$  depending on its heat capacity. In the real case, we observe a logarithmic increase of the sample temperature with time due to an increasing heat exchange  $Q_{ex}$  with the environment, which ends up at a saturation temperature  $T_{max}$  when  $Q_{ex} = Q_M$ . The course can be described well with an exponential fit during the initial period of 20 s as can be seen in Figure 3b. We extract a characteristic time constant of  $\tau = 14.3$  s that is related to the heat exchange  $Q_{ex}$  and therefore to the sample geometry.

## Conclusion

The presented results prove the versatility of the concept of activating large shape-

changes in oriented LCE networks by magnetic heating using a contactless electromagnetic trigger, resulting in a reversible, well-defined change in the relative sample length along the tensor up to 27%. The findings offer the chance to develop a new type of contactless soft actuators.

**Acknowledgements:** We gratefully acknowledge the DFG for financial support within the Emmy Noether program, SPP 1104 and SFB 428. In addition, the *Fonds der Chemischen Industrie* is gratefully acknowledged. We thank Prof. Dr. W. Frank, HHU Düsseldorf, for providing the HF generator, and Dr. R. Thomann, University of Freiburg, for carrying out the TEM-investigations.

- [1] P. G. De Gennes, C. R. *Seances Acad. Sci, Ser. B* **1975**, 281, 101.
- [2] J. Küpfer, H. Finkelmann, *Makromol. Chem. Rapid Commun.* **1991**, 12, 717.
- [3] P. G. DeGennes, M. Hebert, R. Kant, *Macromol. Symp.* **1997**, 113, 39.
- [4] Y. Bar-Cohen, *J. Spacecraft and Rockets* **2002**, 39, 822.
- [5] M. Camacho-Lopez, H. Finkelmann, P. Palffy-Muhoray, M. Shelley, *Nature Mater.* **2004**, 3, 307.
- [6] Y. L. Lu, M. Nakano, A. Shishido, T. Shiono, T. Ikeda, *Chem. Mater.* **2004**, 16, 1637.
- [7] M. Warner, E. Terentjev, *Macromol. Symp.* **2003**, 200, 81.
- [8] W. Lehmann, H. Skupin, C. Tolksdorf, E. Gebhard, R. Zentel, P. Kruger, M. Losche, F. Kremer, *Nature* **2001**, 410, 447.
- [9] S. V. Ahir, A. R. Tajbakhsh, E. M. Terentjev, *Adv. Funct. Mater.* **2006**, 16, 556.

- [10] W. F. Brown, Jr., *J. Appl. Phys. Suppl.* **1959**, 30, 130.
- [11] *Magnetism in Medicine*, Eds., W. Andrä, H. Nowak), Wiley-VCH, Weinheim, Germany 1998.
- [12] A. M. Schmidt, *J. Magnetism Magn. Mater.* **2005**, 289C, 5.
- [13] T. Gelbrich, A. M. Schmidt, *Macromolecules* **2006**, 39, 3469.
- [14] A. Kaiser, T. Gelbrich, A. M. Schmidt, *J. Phys.: Cond. Matter* **2006**, 18, 2563.
- [15] A. M. Schmidt, *Colloid Polym. Sci.* **2007**, 285, 953.
- [16] A. M. Schmidt, *Macromol. Rapid Commun.* **2006**, 27, 1168.
- [17] R. Massart, V. J. Cabuil, *J. Chim. Phys. Chim. Biol.* **1987**, 84, 967.
- [18] A. Kaiser, M. Winkler, S. Krause, H. Finkelmann, A. M. Schmidt, submitted.
- [19] R. Lovell, *Acta Crystallogr. A* **1981**, 37, 135.
- [20] G. R. Mitchell, in: *Orientation in Liquid Crystal Polymers. In Developments in Crystalline Polymers, Vol. 2* (Ed., D. C. Bassett) Elsevier Applied Science, London New York 1988.
- [21] I. Levine, R. B. Zvi, M. Winkler, A. M. Schmidt, M. Gottlieb, *Macromol. Symp.* **2010**, this issue